

Syndrome of occipitoatlantoaxial hypermobility, cranial settling, and Chiari malformation Type I in patients with hereditary disorders of connective tissue

THOMAS H. MILHORAT, M.D.,¹ PAOLO A. BOLOGNESE, M.D.,¹ MISAO NISHIKAWA, M.D.,¹ NAZLI B. McDONNELL, M.D., PH.D.,² AND CLAIR A. FRANCOMANO, M.D.³

¹Department of Neurosurgery, The Chiari Institute, North Shore-Long Island Jewish Health System, Manhasset, New York; ²Medical Genetics, NIH National Institute on Aging; and ³Harvey Institute for Medical Genetics, Greater Baltimore Medical Center, Baltimore, Maryland

Object. Chiari malformation Type I (CM-I) is generally regarded as a disorder of the paraxial mesoderm. The authors report an association between CM-I and hereditary disorders of connective tissue (HDCT) that can present with lower brainstem symptoms attributable to occipitoatlantoaxial hypermobility and cranial settling.

Methods. The prevalence of HDCT was determined in a prospectively accrued cohort of 2813 patients with CM-I. All patients underwent a detailed medical and neuroradiological workup that included an assessment of articular mobility. Osseous structures composing the craniocervical junction were investigated morphometrically using reconstructed 3D computed tomography and plain x-ray images in 114 patients with HDCT/CM-I, and the results were compared with those obtained in patients with CM-I (55 cases) and healthy control individuals (55 cases).

Results. The diagnostic criteria for Ehlers–Danlos syndrome and related HDCT were met in 357 (12.7%) of the 2813 cases. Heritability was generally compatible with a pattern of autosomal dominant transmission with variable expressivity. The diagnostic features of HDCT/CM-I were distinguished from those of CM-I by clinical stigmata of connective tissue disease, a greater female preponderance (8:1 compared with 3:1, $p < 0.001$), and a greater incidence of lower brainstem symptoms (0.41 compared with 0.11, $p < 0.001$), retroodontoid pannus formation (0.71 compared with 0.11, $p < 0.001$), and hypoplasia of the oropharynx (0.44 compared with 0.02, $p < 0.001$). Measurements of the basion–dens interval, basion–atlas interval, atlas–dens interval, dens–atlas interval, clivus–atlas angle, clivus–axis angle, and atlas–axis angle were the same in the supine and upright positions in healthy control individuals and patients with CM-I. In patients with HDCT/CM-I, there was a reduction of the basion–dens interval (3.6 mm, $p < 0.001$), an enlargement of the basion–atlas interval (3.0 mm, $p < 0.001$), and a reduction of the clivus–axis angle (10.8° , $p < 0.001$), clivus–atlas angle (5.8° , $p < 0.001$), and atlas–axis angle (5.3° , $p < 0.001$) on assumption of the upright position. These changes were reducible by cervical traction or returning to the supine position.

Conclusions. The identification of HDCT in 357 patients with CM-I establishes an association between two presumably unrelated mesodermal disorders. Morphometric evidence in this cohort—cranial settling, posterior gliding of the occipital condyles, and reduction of the clivus–axis angle, clivus–atlas angle, and atlas–axis angle in the upright position—suggests that hypermobility of the occipitoatlantal and atlantoaxial joints contributes to retroodontoid pannus formation and symptoms referable to basilar impression. (DOI: 10.3171/SPI-07/12/601)

KEY WORDS • Chiari malformation • connective tissue disorders • cranial settling • craniocervical instability • Ehlers–Danlos syndrome • joint hypermobility

HEREDITARY disorders of connective tissue include a continuum of conditions caused by defects of extracellular matrix elements such as collagens, elastin, or fibrillin.²⁷ The EDSs constitute a distinct category within the HDCT group and are responsible for a wide vari-

Abbreviations used in this paper: CCJ = craniocervical junction; CM-I = Chiari malformation Type I; CT = computed tomography; EDS = Ehlers–Danlos syndrome; HDCT = hereditary disorders of connective tissue; KPS = Karnofsky Performance Scale; MASS = mitral valve, aorta, skeleton, and skin; MR = magnetic resonance; POTS = postural orthostatic tachycardia syndrome; SD = standard deviation; TGF β = transforming growth factor- β .

ety of systemic manifestations including joint hypermobility, recurrent joint dislocations, skin laxity and fragility, poor wound healing, widened atrophic scars, tendon and muscle rupture, kyphoscoliosis, uterine rupture, large hernias, vascular fragility, easy bruising, venous varices, arteriovenous fistulas, aortic dilation, and arterial rupture.^{2–4,9,10,24,37,43,47} Despite a recently revised nosology for EDS,² a significant number of cases cannot be precisely classified. Some of these patients have an overlap disorder in which there are features of both EDS and Marfan syndrome. Other individuals have some features of Marfan syndrome, but other features fail to meet Ghent criteria and are classified

as a MASS phenotype.¹⁰ Marfan syndrome is distinguished by cardiovascular defects including mitral valve prolapse, aortic aneurysms that tend to rupture, skeletal abnormalities such as arachnodactyly and long limbs (dolichostenomelia), pectus deformity, dural ectasia, and ectopia lentis. There are scant data on the prevalence of HDCT except for EDS and Marfan syndrome, which are estimated to occur in one per 5000 to 10,000 individuals.⁶ The most common types of HDCT are inherited dominantly.^{2-4,10,23,37,39,43,47}

Chiari malformations include a heterogeneous group of hindbrain disorders that are characterized by herniation of the cerebellar tonsils through the foramen magnum. There is accumulating evidence that CM-I, the most common type, is a disorder of the paraxial mesoderm caused by underdevelopment of the posterior cranial fossa, overcrowding of the normally developed hindbrain, and downward herniation of the cerebellar tonsils.^{1,25,26,28,31,32,42,49} The prevalence of CM-I is estimated to be in the range of one per 1000 to one per 5000 individuals.⁴⁶ Familial transmission can occur by autosomal recessive inheritance or autosomal dominant inheritance with incomplete penetrance, but most cases occur sporadically.^{28,46}

The impetus for this study was our experience with patients referred for the evaluation of failed CM surgery before 2002. Included in this cohort was a subset of patients with HDCT in which varying degrees of craniocervical instability seemed to be related to underlying joint hypermobility. To better understand the relationship of HDCT and CM-I, we analyzed a prospectively enrolled cohort of patients with CM-I to characterize the clinical features, radiographic/imaging findings, and genetic aspects of the combined disorder.

Clinical Material and Methods

Study Population

The population was composed of 2813 patients with MR imaging–confirmed CM-I who were evaluated consecutively between January 2002 and April 2007. A total of 1262 patients (45%) had been referred for evaluation after failed CM surgery. There were 2127 females and 686 males who ranged in age from 2 to 88 years (mean age 30.9 ± 4.0 years [\pm SD]).

Assessment Tools

A database (Microsoft Office Access 2007) that included a detailed medical history, family history, and checklist of symptoms and signs was established for each patient. A questionnaire was developed to elicit information on the family history and features of HDCT and CM-I. All patients underwent a physical examination, complete neurological examination, cervical MR imaging, and measurement of articular mobility. Additional information was provided in some patients by whole-neuraxis MR imaging, CT of the head with 2D and 3D reconstructions, cine-MR imaging, standup MR imaging, flexion and extension radiography of the cervical spine, CT scanning of the spine, barium swallow, 24-hour sleep monitoring, continuous cardiac monitoring, electrocardiography, echocardiography, tilt-table testing, audiography, vestibular function tests, and neuropsychological assessments. The clinical disability of

each patient was measured using the KPS, with scores ranging from 0 to 100.³⁰

Joint hypermobility was assessed using the Beighton score.² The scores were assigned as follows: 1) passive dorsiflexion of the little fingers of each hand beyond 90° (one point for each hand); 2) passive opposition of the thumbs to the flexor aspect of the forearm (one point for each hand); 3) hyperextension of the elbows beyond 10° (one point for each elbow); 4) hyperextension of the knees beyond 10° (one point for each knee); and 5) forward flexion of the trunk with the knees fully extended so that the palms of the hands rest flat on the floor (one point). A Beighton score of 5 or more was defined as a positive test for joint hypermobility in postpubertal persons. Tissue fragility was defined as the presence of one or more of the following findings: 1) easy bruising; 2) history of poor wound healing; and 3) dystrophic scars exhibiting a thin and atrophic (papyraceous) appearance. Features of marfanoid habitus such as tall stature and long limbs, arachnodactyly, asthenic appearance with low body fat, long thin face with malar hypoplasia, down-slanting palpebral fissures, pectus deformity, and scoliosis were noted on clinical examination. The diagnosis of EDS and other HDCT was established on the basis of the Beighton score, clinical examination, family history, and supplementary tests including echocardiography, MR imaging or CT angiography of the chest, abdomen and pelvis, bone densitometry, and skin biopsy for analysis of collagens.

In cases in which the disorder could not be classified precisely, the classification was considered to represent an “overlap phenotype” if six or more of the following criteria were met: 1) Beighton score of 3 or more; 2) tissue fragility with poor wound healing; 3) spontaneous large-joint dislocations; 4) mitral valve prolapse; 5) mitral, tricuspid, or pulmonic valve regurgitation; 6) POTS; 7) orthostatic hypotension; and 8) marfanoid appearance without meeting Ghent criteria.

The clinical and radiographic/imaging criteria for establishing the diagnosis of CM-I have been previously described.²⁸ For the purposes of this study, we adopted the narrow but widely accepted definition of CM-I as tonsillar herniation of 5 mm or greater below the foramen magnum.⁸ We defined minimal tonsillar herniation as tonsillar descent of 5 to 7 mm below the foramen magnum. Tonsillar descent of 0 to 4 mm was defined as low-lying cerebellar tonsils.

Patients in whom there was clinical suspicion of craniocervical instability underwent a trial of invasive cervical traction. Cranial tongs were applied in the operating room after propofol sedation and injection of a local anesthetic. After the patient had awakened fully, invasive cervical traction was performed with the patient sitting in an 80° Fowler position. Using graduated weights, the head was extracted on the neck under fluoroscopic guidance, and a checklist of symptoms and neurological findings obtained immediately before testing was assessed as the extraction proceeded. Once an optimum level of relief had been achieved, permanent fluoroscopic images were obtained to compare morphometric measurements of osseous structures at the CCJ in the supine, upright (sitting), and extracted positions. The invasive cervical traction test was defined as positive if optimal extraction produced an 80% or greater relief of baseline symptoms and signs.

Morphometric Analysis of the CCJ

Using reconstructed 2D sagittal CT scans and plain x-ray films, the osseous components of the CCJ were measured in 114 patients with HDCT/CM-I, 55 age- and sex-matched patients with CM-I and no evidence of HDCT, and 55 age- and sex-matched healthy control individuals. The selection process was limited to patients with HDCT/CM-I and CM-I who had undergone invasive cervical traction for assessment of craniocervical stability immediately before a planned surgical procedure. Morphometric measurements in the two cohorts were compared in the supine, upright (sitting), and extracted positions.

Occipitoatlantal motion was measured using the method described by Wiesel and Rothman⁵⁰ with some modification; occipitoaxial motion was measured using the method described by Harris and colleagues^{14,15} with some modification; and atlantoaxial motion was measured using the method described by Ranawat et al.⁴¹ with some modification. We established a means for assessing occipitoatlantoaxial motion by combining these methods with new measurements developed by us (Figs. 1 and 2). We measured the interval between the basion and top of dens (basion-dens interval), the interval between the basion and plane of the posterior surface of the atlantal anterior arch (basion-atlas interval), the interval between the posterior surface of the atlantal anterior arch and the dens (atlas-dens interval), and the interval between the top of the dens and a line drawn between the lowest point of the atlantal anterior arch and the lowest point of the atlantal posterior arch (dens-atlas interval). The following lines were established to assess osseous relationships: Line A, the plane of the posterior surface of the anterior arch of the atlas; Line B, that between the lowest point of the anterior arch of the atlas and the lowest point of the posterior arch of the atlas; Line C, the superior plane of the clivus; Line D, the plane of the

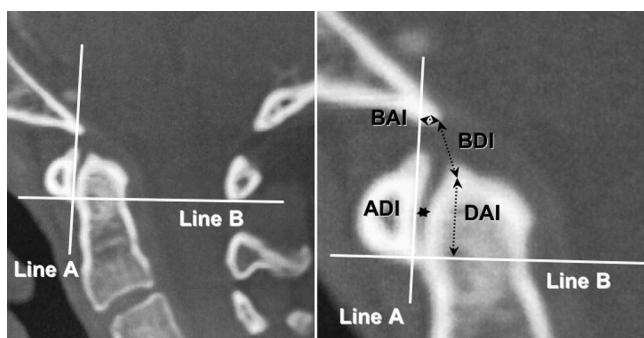


FIG. 1. Midsagittal reconstructed 2D CT scans obtained in control individuals with normal anatomy, showing lines (left) and measurement intervals (right) for assessing osseous structures at the CCJ: Line A, plane of posterior surface of anterior arch of atlas; Line B, that between lowest point of anterior arch of atlas and lowest point of posterior arch of atlas. Arrowheads identify the basion-atlas interval; upper arrow with dotted lines defines the basion-dens interval; lower arrow with dotted lines indicates the interval between the dens and Line B (the atlas-dens interval); and the star identifies atlas-dens interval. ADI = interval between posterior surface of anterior arch of atlas and dens; BAI = interval between basion and Line A; BDI = interval between basion and top of dens; DAI = interval between top of dens and Line B.

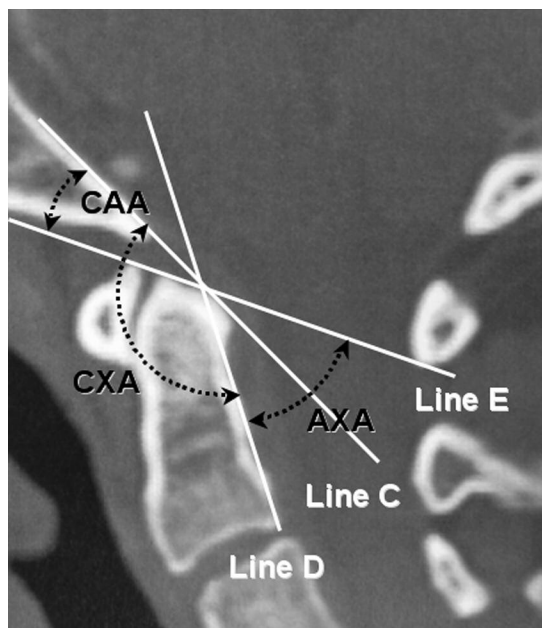


FIG. 2. Lines and angles for assessing osseous structures at the CCJ on midsagittal reconstructed 2D CT scans in control individuals with normal anatomy: Line C, superior plane of the clivus; Line D, plane of posterior surface of dens; and Line E, that between the top of anterior arch of atlas and lowest point of posterior arch of atlas. AXA = angle between atlas (Line E) and axis (Line D); CAA = angle between clivus (Line C) and atlas (Line E); CXA = angle between clivus (Line C) and axis (Line D).

posterior surface of the dens; and Line E, that between the top of the atlas and lowest point of the posterior arch of the atlas. We calculated the angle between the atlas and axis (angle between Line E and Line D [atlas-axis angle]), the angle between the clivus and atlas (angle between Line C and Line E [clivus-atlas angle]), and the angle between the clivus and axis (angle between Line C and Line D [clivus-axis angle]).

Statistical Analysis

Statistical analyses of clinical data were performed with SPSS for Windows (version 15.0; SPSS, Inc.). Mean values are presented \pm SDs. In the HDCT/CM-I and CM-I cohorts, the mean differences in age, age at onset of symptoms, and KPS score at the time of clinical presentation were assessed using independent-sample Student t-tests. Categorical data were analyzed using two-by-two contingency tables, from which chi-square values were calculated, and the corresponding probability values were established. Analyses of morphometric data were performed with SPSS for Macintosh (version 13.0). The incidence of associated abnormalities was analyzed using the chi-square test. Demographic differences between patients and healthy control individuals were tested with the nonparametric Mann-Whitney U-test. Comparisons of data with patients in the supine, sitting, and traction positions were tested with analysis of variance. The distribution of the data was analyzed using the F-test. Significance was indicated by a two-tailed probability value of less than 0.01.

TABLE 1

*Characteristics of patients with CM-I with and without HDCT**

Variable	Patient Group (%)	
	HDCT/CM-I	CM-I
total no. of cases	357	2456
mean age of symptom onset (yrs)	13.3 ± 4.6	22.0 ± 3.1
mean age at presentation (yrs)	25.7 ± 4.3	31.7 ± 3.9
sex		
male	39 (11)	647 (26)
female	318 (89)	1809 (74)
no prior op	232 (65)	1319 (54)
failed CM op	125 (35)	1137 (46)
classification of HDCT		
hypermobile EDS	149 (42)	
classic EDS	96 (27)	
arthrochlasia EDS	5 (1)	
Marfan syndrome	17 (5)	
MASS phenotype	19 (5)	
overlap disorder	71 (20)	

* Mean values are presented with ± SDs.

Results

Characteristics of Patients

The diagnostic criteria for HDCT were met in 357 (12.7%) of 2813 patients with CM-I. As shown in Table 1, patients with HDCT tended to be younger, exhibited a greater female preponderance, and had earlier-onset symptoms than those with CM-I. One hundred twenty-five patients (35%) with HDCT/CM-I had a history of failed Chiari surgery. Using the current nosology for EDS and related disorders,^{2,10,23,37,47} HDCT types were classified as follows: 1) EDS, hypermobility type (149 patients); 2) EDS, classical type (96 patients); 3) EDS, arthrochlasia type (five patients); 4) Marfan syndrome (17 patients); 5) MASS phenotype (19 patients); and 6) overlap disorder (71 patients). Other genetic conditions encountered in the HDCT/CM-I cohort included VACTERL (vertebral, anal, cardiac, tracheoesophageal fistula, renal, limb) syndrome (six patients), achondroplasia (four patients), osteogenesis imperfecta (two patients), osteopetrosis (one patient), and Noonan syndrome (one patient).

Analysis of Family History

Reliable family history information was available in 139 probands with HDCT/CM-I (Table 2). Patients with Marfan syndrome were not included in this analysis. The family history was considered positive only if the diagnosis had been made by a physician. It is likely that the number of relatives with HDCT is underrepresented because the diagnosis can be elusive without a clinical genetics evaluation. Forty-four probands (32%) had at least one first-degree relative with CM-I, and 30 probands (22%) had at least one first-degree relative with HDCT. In one case, the only affected relative was an identical twin. Twenty-two probands (16%) had CM-I and HDCT descending through the same lineage, compatible with an autosomal dominant pattern of inheritance. All but two families seemed to have descended through the maternal lineage. Only one proband had both disorders descending through separate lineages.

TABLE 2

Familial aggregation of CM-I and HDCT in first-degree relatives of patients with both conditions

Variable	No. of Patients (%)
total no. of probands w/ HDCT/CM-I	139 (100)
probands having relatives w/ CM-I	44 (32)
1 affected relative	24 (17)
>1 affected relative	20 (14)
total no. of affected relatives	72 (52)
probands having relatives w/ HDCT	30 (22)
1 affected relative	13 (9)
>1 affected relative	17 (12)
total no. of affected relatives	43 (31)
probands w/ HDCT/CM-I in same lineage	22 (16)
probands w/ HDCT/CM-I in separate lineages	1 (<1)

Clinical Presentation of Patients

Variations in the clinical presentation of patients with HDCT/CM-I are given in Table 3. Compared with patients with CM-I, those with the combined disorder experienced a greater incidence of lower brainstem symptoms including

TABLE 3

Diagnostic distinctions of CM-I in patients with and without HDCT

Variable	Patient Group (%)		
	HDCT/CM-I	CM-I	p Value
total no. of cases	357	2456	
symptoms & signs			
nausea	239 (67)	343 (14)	<0.001
dysphagia	246 (69)	639 (26)	<0.001
throat tightness	171 (48)	221 (9)	<0.001
shortness of breath	96 (27)	98 (4)	<0.001
sleep apnea	110 (31)	270 (11)	<0.001
palpitations	218 (61)	514 (21)	<0.001
facial pain	89 (25)	172 (7)	<0.001
double vision	93 (26)	123 (5)	<0.001
syncope	50 (14)	25 (1)	<0.001
diagnostic findings			
Lhermitte sign	246 (69)	74 (3)	<0.001
Raynaud phenomenon	136 (38)	170 (7)	<0.001
downward nystagmus	54 (15)	73 (3)	<0.001
dizziness w/ head turning	133 (37)	196 (8)	<0.001
orthostatic hypotension*	74 (21)	49 (2)	<0.001
postural orthostatic tachycardia syndrome*	92 (26)	123 (5)	<0.001
supraventricular tachycardia†	114 (32)	269 (11)	<0.001
mitral valve prolapse‡	174 (49)	74 (3)	<0.001
mitral valve regurgitation‡	35 (10)	49 (2)	<0.001
radiographic findings			
retroodontoid pannus w/ basilar impression	253 (71)	270 (11)	<0.001
cervical disc disease	207 (58)	295 (12)	<0.001
cervical spine subluxation	67 (19)	48 (2)	<0.001
scoliosis	175 (49)	539 (22)	<0.001
temporomandibular joint disease	231 (65)	419 (17)	<0.001
oropharynx hypoplasia	158 (44)	50 (2)	<0.001
hypertrophy of styloid process	114 (32)	244 (10)	<0.001
mean KPS score§	67.5 ± 3.9	76.8 ± 3.4	<0.001

* Confirmed by tilt-table test.

† Confirmed by Holter monitor.

‡ Confirmed by echocardiography.

§ Mean values are presented with SDs.

Chiari malformation Type I and connective tissue disorders

nausea, dysphagia, throat tightness, shortness of breath, sleep apnea, palpitations, facial pain, double vision, and syncope ($p < 0.001$). Diagnostic distinctions included an increased incidence of Lhermitte sign, Raynaud phenomenon, downward nystagmus, dizziness with head turning, supraventricular tachycardia, POTS, orthostatic hypotension, mitral valve prolapse, and mitral valve regurgitation ($p < 0.001$). The mean KPS score in the HDCT/CM-I cohort (67.5 ± 3.9) was lower than that in the CM-I cohort (76.8 ± 3.4 , $p < 0.001$). Imaging distinctions included an increased incidence of retroodontoid pannus formation of 3 mm or greater with basilar impression, cervical disc disease, cervical spine subluxation, scoliosis, hypertrophy of the styloid processes, temporomandibular joint disease, and oropharynx hypoplasia ($p < 0.001$).

Morphometric Analyses and Operative Positions

Morphometric measurements of the CCJ with the patient in the supine position demonstrated no significant differences in the basion–dens interval, basion–atlas interval, atlas–dens interval, dens–atlas interval, clivus–atlas angle, clivus–axis angle, and atlas–axis angle in patients with HDCT/CM-I, patients with CM-I, and healthy control individuals (Table 4). There were no significant changes from baseline measurements in patients with CM-I on assumption of the upright (sitting) position or during invasive cervical traction with extraction weights of 20 to 35 lb. In patients with HDCT/CM-I, however, assumption of the upright (sitting) position resulted in a reduction of the basion–dens interval from a mean of 7.7 to 4.1 mm ($p < 0.001$; Fig. 3); posterior gliding of the occipital condyles with an increase of the basion–atlas interval from a mean of 2.0 to 5.0 mm ($p < 0.001$; Fig. 4); anterior flexion of the occipitoatlantal joint, as demonstrated by a decrease of the clivus–atlas angle, clivus–axis angle, and atlas–axis angle by a mean of 5.8° ($p < 0.001$), 10.8° ($p < 0.001$), and 5.3° ($p < 0.001$), respectively (Fig. 5); anterior flexion of the atlas over the axis, as demonstrated by a reduction of the atlas–axis angle (mean 5.3° , $p < 0.001$); and change in the atlas–dens interval in flexion and extension (mean 1.8 mm, $p < 0.001$). Vertical (sitting) MR imaging helped to show the dynamic features of occipitoatlantoaxial hypermobility and functional cranial settling (Fig. 6). These abnormalities were reducible by traction (Figs. 3–5) or a return to the supine position.

Discussion

The identification of HDCT in 357 patients with CM-I establishes an association of two mesodermal disorders that have a predicted coincidence of one per five to 10,000,000 individuals. Previous evidence of this association has been limited to anecdotal reports of CM-I occurring in patients with Marfan syndrome^{5,35,38,39} and the newly described Loeys–Dietz syndrome.²³ The rate of concurrence of HDCT and CM-I in this study (12.7%) was clearly biased by the disproportionate number of patients referred for evaluation of failed CM surgery, HDCT, and craniocervical instability. Well-designed epidemiological studies are needed to establish the true prevalence of the combined disorder.

Family history data provided strong support for a causal relationship of HDCT and CM-I. In the HDCT/CM-I

TABLE 4
Morphometric measurements of osseous structures at CCJ in patients with CM-I with and without HDCT*

Variable	Patient Group (%)		
	Healthy Controls	CM-I	HDCT/CM-I
no. of patients	55	55	114
sex			
male	14 (25.5)	12 (21.8)	17 (14.9)
female	41 (74.5)	43 (78.2)	97 (85.1)
mean age (yrs)	37.6 ± 8.7	38.2 ± 11.5	33.1 ± 9.76
basion–dens interval (mm)			
supine	7.4 ± 1.58	7.5 ± 1.75	7.7 ± 1.85
sitting	7.2 ± 1.59	7.2 ± 1.88	4.1 ± 1.82†‡
traction	NA	7.8 ± 2.01	10.8 ± 2.53‡§
basion–atlas interval (mm)			
supine	1.8 ± 1.21	1.8 ± 1.24	2.0 ± 1.22
sitting	2.1 ± 1.88	2.1 ± 1.78	5.0 ± 1.48†‡
traction	NA	1.4 ± 1.10	1.5 ± 1.24§
dens–atlas interval (mm)			
supine	12.3 ± 2.17	12.4 ± 2.72	12.7 ± 2.58
sitting	12.5 ± 2.00	12.7 ± 2.52	13.1 ± 3.12
traction	NA	11.9 ± 2.87	10.0 ± 2.72‡§
atlas–dens interval (mm)			
supine	1.5 ± 0.55	1.5 ± 0.50	1.6 ± 0.58
sitting	1.5 ± 0.57	1.6 ± 0.60	2.1 ± 1.11
traction	NA	1.5 ± 0.55	2.0 ± 1.25
flexion	1.7 ± 0.75	1.7 ± 0.70	3.3 ± 0.80
extension	1.5 ± 0.57	1.4 ± 0.60	1.5 ± 0.75
change w/ flexion/extension	0.2 ± 0.20	0.3 ± 0.30	1.8 ± 0.70†
clivus–atlas angle (°)			
supine	37.9 ± 7.14	38.0 ± 6.98	38.3 ± 6.35
sitting	36.5 ± 7.52	37.3 ± 7.15	32.5 ± 6.14†‡
traction	NA	35.2 ± 7.17	42.5 ± 7.87‡§
clivus–axis angle (°)			
supine	147.6 ± 6.61	148.5 ± 5.87	151.8 ± 6.00
sitting	147.8 ± 6.00	147.7 ± 5.77	141.0 ± 7.22†‡
traction	NA	151.8 ± 5.85	164.8 ± 6.74‡§
atlas–axis angle (°)			
supine	56.8 ± 4.71	56.5 ± 4.74	55.7 ± 5.41
sitting	55.0 ± 4.88	55.7 ± 4.84	50.4 ± 5.62†‡
traction	NA	55.6 ± 4.95	57.1 ± 5.72§

* Where applicable, values are expressed as the means ± SDs. Abbreviation: NA = not applicable.

† Significant differences compared with patients with CM-I and healthy control groups ($p < 0.001$).

‡ Significant differences compared with supine position ($p < 0.001$).

§ Significant differences compared with sitting position ($p < 0.001$).

cohort, the aggregation of CM-I in 32% of families was greater than that reported in families with CM-I alone,^{28,46} and there was a positive family history of HDCT in 22% of probands. A positive family history of HDCT/CM-I through the same lineage was present in 16% of probands. Given that HDCT and CM-I are often underdiagnosed, the actual numbers of affected relatives with either or both disorders may be underestimated. The pattern of transmission of HDCT/CM-I was generally compatible with autosomal dominant inheritance with variable expressivity.

Mutations of TGFβ₁ or TGFβ₂ receptors have been described recently in patients with a new connective tissue disorder characterized by early and aggressive aneurysms of the aorta.²³ Two of 10 patients were found to have CM-I. Histological abnormalities occurring with TGFβ₂

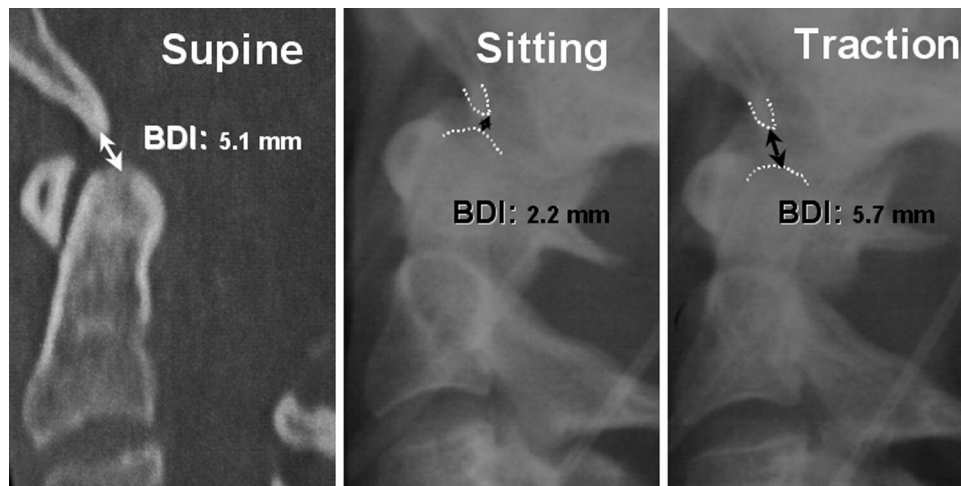


FIG. 3. Evidence of functional cranial settling in a 25-year-old woman with HDCT/CM-I. *Left:* The results of midsagittal reconstructed 2D CT scanning in the supine position indicated a baseline basion–dens interval of 5.1 mm. *Center and Right:* The results of plain radiography indicated a decrease of the basion–dens interval (2.2 mm) in the sitting position and an increase of the basion–dens interval (5.7 mm) during traction with a 20-lb weight.

receptor mutations include a loss of elastin and disarrayed elastic fibers similar to the findings in patients with fibrillin mutations that have been implicated in Marfan syndrome and the MASS phenotype.²³ Evidence that a conditional knockout of TGFβ₂ receptor in neural crest cells causes defects of the calvaria in a mouse model¹⁷ lends plausibility to the hypothesis that abnormalities of the extracellular matrix can lead to abnormalities of osseous development of the skull.

From a clinical standpoint, patients with HDCT/CM-I tended to present with typical diagnostic features of CM-I.

Obvious stigmata of an underlying connective tissue disorder were not always evident, and a detailed workup that included an assessment of dysmorphic features by a geneticist, assessment of articular mobility by a rheumatologist, and a variety of supplementary tests was sometimes needed to establish the correct diagnosis. A distinctive feature of the clinical presentation was the greater incidence of lower brainstem symptoms such as nausea, dysphagia, sleep apnea, POTS, and orthostatic hypotension. The predominance of these symptoms was reflected by the lower KPS scores in the HDCT/CM-I cohort (mean score 67.5 ±

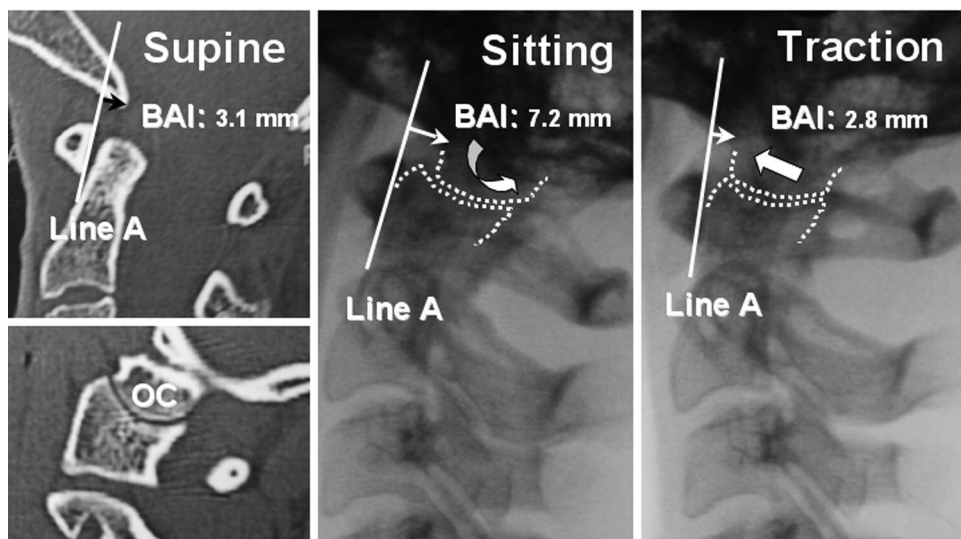


FIG. 4. Evidence of posterior gliding of the occipital condyle in a 33-year-old woman with HDCT/CM-I. Results of midsagittal reconstructed 2D CT scanning with the patient in the supine position, showing baseline basion–atlas interval of 3.1 mm (*upper left*) and normal articulation of occipital condyle (OC) (*lower left*). Results of plain radiography (*center and right*) show an increase of the basion–atlas interval (7.2 mm) in the sitting position and a decrease of the basion–atlas interval (2.8 mm) during traction with a 20-lb weight. The occipitoatlantal joint (outlined by dotted line) glides posteriorly in the sitting position (*curved arrow*) and is reduced by traction (*thick arrow*). Line A, plane of the posterior surface of the anterior arch of the atlas.

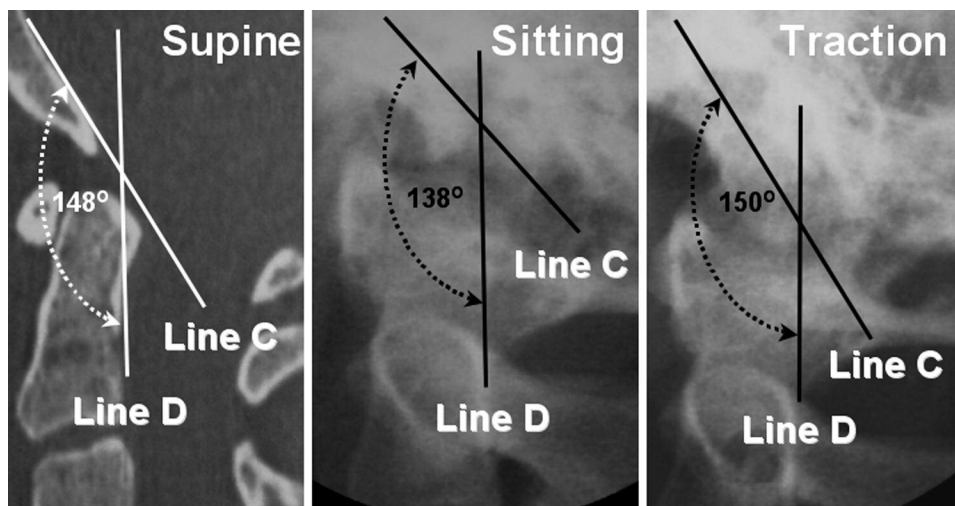


FIG. 5. Evidence of anterior flexion of occipital condyles in a 41-year-old woman with HDCT/CM-I. Results of mid-sagittal reconstructed 2D CT scanning in supine position (*left*) indicate baseline clivus–axis angle of 148°. Results of plain radiography (*center* and *right*) indicate a decrease of the clivus–axis angle (138°) in the sitting position and an increase of the clivus–axis angle (150°) during traction with a 20-lb weight. *Line C*, superior plane of clivus; *Line D*, plane of posterior surface of dens. Angle between clivus (*Line C*) and axis (*Line D*).

3.9) compared with those in the CM-I cohort (mean score 76.8 ± 3.4) and by the need for some patients to lead a sedentary or even bed-confined life to minimize symptoms.

The most distinctive imaging finding in this study was the presence of a retroodontoid pannus of at least 3.0 mm with varying degrees of basilar impression in 71% of patients with HDCT/CM-I, compared with 11% of patients with CM-I. Retroodontoid pannus formation is a common finding in patients with rheumatoid arthritis^{7,13,33,44,54} and has

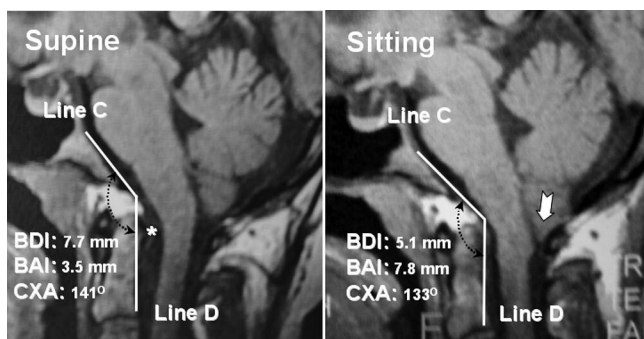


FIG. 6. Results of vertical MR imaging in a 27-year-old woman with HDCT/CM-I. Midsagittal image in supine position (*left*) showing normal basion–dens interval (7.7 mm), normal basion–atlas interval (3.5 mm), normal clivus–axis angle (141°), large retroodontoid pannus, and low-lying cerebellar tonsils. On assumption of the upright position (*right*), there is evidence of cranial settling (2.6 mm decrease of basion–dens interval), posterior gliding of occipital condyles (4.3 mm increase of basion–atlas interval), anterior flexion of the occipitoatlantal joint (8° decrease of clivus–axis angle), increased basilar impression, and cerebellar ptosis with downward displacement of cerebellar tonsils to C-1 (*white arrow*). Note the greatly increased impaction of the foramen magnum anteriorly and posteriorly. *Line C*, superior plane of the clivus; *Line D*, plane of the posterior surface of the dens. *Asterisk* indicates the retroodontoid pannus.

been reported in association with chronic atlantoaxial subluxation,^{11,16,52} nonunion odontoid fractures,^{20,48} os odontoid-eum,¹⁸ gout and pseudogout (calcium pyrophosphate dehydrate deposition),^{21,53} villonodular synovitis,¹⁹ synovial cysts,^{29,34} and Forestier disease.^{12,36} Although the mechanisms underlying pannus formation have yet to be elucidated, pathological factors that appear to be common to all inflammatory, traumatic, and metabolic conditions associated with this lesion include the following: 1) damage of ligaments that support and limit motion of the atlantoaxial joint; 2) hypermobility of the atlantoaxial joint with increased motion of the odontoid; and 3) disruption of the transverse, alar, and apical ligaments with atlantoaxial subluxation.^{14,15,40} Reports of pannus resolution or reduction in size after atlantoaxial¹⁸ or occipitocervical fusion^{51,54} provide indirect evidence that the instability of the atlantoaxial joint is a proximate cause of retroodontoid pannus formation.

In this study, morphometric measurements of osseous structures forming the CCJ were made on reconstructed 2D CT scans and plain x-ray films. Magnetic resonance imaging measurements were excluded because of the inability to define bone edges precisely. Standard measurements included the basion–dens interval, for evaluating the vertical relationship of the clivus and odontoid;^{14,15,50} the atlas–dens interval, for evaluating the horizontal relationship of the odontoid and anterior arch of the atlas;^{22,40} and the clivus–axis angle, for evaluating the angle between the clivus and odontoid.⁴⁵ New measurements that we developed for investigating motion of the occipitoatlantoaxial complex included the basion–atlas interval, for evaluating the horizontal relationship of the clivus and anterior arch of the atlas; the dens–atlas interval, for evaluating the vertical relationship of the odontoid and atlas; the atlas–axis angle, for evaluating the angle between the atlas and axis; and the clivus–atlas angle, for evaluating the angle between the clivus and atlas.

As shown in Table 4, there were no significant differ-

ences in the seven baseline measurements of patients with HDCT/CM-I, patients with CM-I, and in healthy control individuals in the supine position or in patients with CM-I in the upright (sitting) position or during traction. Baseline measurements of the basion–dens interval, atlas–dens interval, and clivus–axis angle were consistent with previously published values.^{14,15,22,40,45,50} In patients with HDCT/CM-I, assumption of the upright (sitting) position resulted in hypermobility of the occipitoatlantoaxial complex and cranial settling. Hypermobility of the occipitoatlantal joint was shown by posterior gliding of the occipital condyles, as demonstrated by an increase of the basion–atlas interval (mean 3.0 mm, $p < 0.001$) and by anterior flexion of the occipitoatlantal joint, as demonstrated by a reduction of the clivus–atlas angle and clivus–axis angle by a mean of 5.8° ($p < 0.001$) and 10.8° ($p < 0.001$), respectively. Hypermobility of the atlantoaxial joint was shown by anterior flexion of the atlas over the axis, as demonstrated by a reduction of the atlas–axis angle (mean 5.3° , $p < 0.001$) and by change of the atlas–dens interval in flexion and extension (mean 1.8 mm, $p < 0.001$). Reduction of the basion–dens interval in the upright position (mean 3.6 mm, $p < 0.001$) established the diagnosis of functional cranial settling.

The term “functional cranial settling” has been introduced to describe a reduction of the distance between the basion and odontoid (basion–dens interval) that occurs only in the upright position and is not caused by bone and cartilage destruction. Functional cranial settling is probably caused by one or both of the following mechanisms: 1) laxity of ligaments supporting the occipitoatlantal joint, resulting in posterior gliding of the occipital condyles and reduction of the clivus–axis angle; or 2) generalized laxity of connective tissue structures at the CCJ including the cruciate ligament, the tectorial membrane, and supporting ligaments of the atlantoaxial joint, sufficient to permit upward migration of the odontoid process. The observation that functional cranial settling and reduction of the basion–dens interval can be reduced by cervical traction or returning the patient to the supine position seems to rule out significant bone and cartilage damage of the occipitoatlantoaxial complex in this group of patients.

Recent experience with vertical MR imaging has proved helpful in understanding the dynamic features of occipitoatlantoaxial hypermobility. As shown in Fig. 6, functional cranial settling was associated with notable displacements that included reduction of the basion–dens interval, posterior gliding of the occipital condyles, anterior flexion of the occipitoatlantal joint, increased basilar impression, and cerebellar ptosis with downward displacement of the cerebellar tonsils. These displacements are consistent with the often-pronounced symptoms and signs of lower brainstem dysfunction experienced by patients with cranial settling on assumption of the upright position.

Conclusions

In this report, we described a previously unrecognized association of CM-I and HDCT. We found that patients with the combined disorder exhibit varying degrees of occipitoatlantoaxial hypermobility that results in functional cranial settling, caudal displacement of the cerebellar

tonsils, retroodontoid pannus formation, and symptoms referable to basilar impression.

Acknowledgment

We thank Dr. Raymond V. Damadian (Fonar Corporation) for providing technical assistance and supervision of patients undergoing vertical MR imaging.

References

1. Badie B, Mendoza D, Batzdorf U: Posterior fossa volume and response to suboccipital decompression in patients with Chiari I malformation. *Neurosurgery* **37**:214–218, 1995
2. Beighton P, De Paepe A, Steinmann B, Tsipouras P, Wenstrup RJ: Ehlers-Danlos syndromes: revised nosology, Villefranche, 1997. Ehlers-Danlos National Foundation (USA) and Ehlers-Danlos Support Group (UK). *Am J Med Genet* **77**:31–37, 1998
3. Beighton PH (ed): *McKusick's Heritable Disorders of Connective Tissue*, ed 5. St. Louis: Mosby Co, 1999, pp 189–253
4. Beighton PH, Horan FT: Dominant inheritance in familial generalised articular hypermobility. *J Bone Joint Surg Br* **52**: 145–147, 1970
5. Braca J, Hornyak M, Murali R: Hemifacial spasm in a patient with Marfan syndrome and Chiari I malformation. Case report. *J Neurosurg* **103**:552–554, 2005
6. Byers PH: Disorders of collagen biosynthesis and structure, in Scriver CR, Sly WS, Childs B, Beaudet AL, Valle D, Kinzler KW, et al (eds): *The Metabolic and Molecular Bases of Inherited Disease*, ed 8. Edinburgh: Churchill Livingstone, 2001, pp 1065–1081
7. Dvorak J, Grob D, Baumgartner H, Gschwend N, Grauer W, Larsson S: Functional evaluation of the spinal cord by magnetic resonance imaging in patients with rheumatoid arthritis and instability of upper cervical spine. *Spine* **14**:1057–1064, 1989
8. Elster AD, Chen MY: Chiari I malformations: clinical and radiologic reappraisal. *Radiology* **183**:347–353, 1992
9. Gilchrist D, Schwarze U, Shields K, MacLaren L, Bridge PJ, Byers PH: Large kindred with Ehlers-Danlos syndrome type IV due to a point mutation (G571S) in the COL3A1 gene of type III procollagen: low risk of pregnancy complications and unexpected longevity in some affected relatives. *Am J Med Genet* **82**: 305–311, 1999
10. Glesby MJ, Pyeritz RE: Association of mitral valve prolapse and systemic abnormalities of connective tissue. A phenotypic continuum. *JAMA* **262**:523–528, 1989
11. Goel A, Phalke U, Cacciola F, Muzumdar D: Atlantoaxial instability and retroodontoid mass—two case reports. *Neurol Med Chir* **44**:603–606, 2004
12. Goffin J, Van Calenbergh F: Forestier's disease. *J Neurosurg* **85**: 524–525, 1996
13. Grob D, Wursch R, Grauer W, Sturzenegger J, Dvorak J: Atlantoaxial fusion and retrodental pannus in rheumatoid arthritis. *Spine* **22**:1580–1584, 1997
14. Harris JH Jr, Carson GC, Wagner LK: Radiologic diagnosis of traumatic occipitovertebral dissociation: 1. Normal occipitovertebral relationships on lateral radiographs of supine subjects. *AJR Am J Roentgenol* **162**:881–886, 1994
15. Harris JH Jr, Carson GC, Wagner LK, Kerr N: Radiologic diagnosis of traumatic occipitovertebral dissociation: 2. Comparison of three methods of detecting occipitovertebral relationships on lateral radiographs of supine subjects. *AJR Am J Roentgenol* **162**: 887–892, 1994
16. Isono M, Ishii K, Kamida T, Fujiki M, Goda M, Kobayashi H: Retro-odontoid soft tissue mass associated with atlantoaxial subluxation in an elderly patient: a case report. *Surg Neurol* **55**: 223–227, 2001
17. Ito Y, Yeo JY, Chytil A, Han J, Bringas P Jr, Nakajima A, et al: Conditional inactivation of Tgfb β 2 in cranial neural crest causes

Chiari malformation Type I and connective tissue disorders

- cleft palate and calvaria defects. **Development** **130**:5269–5280, 2003
18. Jun BY: Complete reduction of retro-odontoid soft tissue mass in os odontoideum following the posterior C1–C2 transarticular screw fixation. **Spine** **24**:1961–1964, 1999
 19. Kleinman GM, Dagi TF, Poletti CE: Villonodular synovitis in the spinal canal: case report. **J Neurosurg** **52**:846–848, 1980
 20. Lansen TA, Kasoff SS, Tenner MS: Occipitocervical fusion for reduction of traumatic periodontoid hypertrophic cicatrix. Case report. **J Neurosurg** **73**:466–470, 1990
 21. Leaney BJ, Calvert JM: Tophaceous gout producing spinal cord compression. Case report. **J Neurosurg** **58**:580–582, 1983
 22. Levine AM, Edwards CC: Traumatic lesions of the occipitoatlantoaxial complex. **Clin Orthop Relat Res** **239**:53–68, 1989
 23. Loeyes BL, Chen J, Neptune ER, Judge DP, Podowski M, Holm T, et al: A syndrome of altered cardiovascular, craniofacial, neurocognitive and skeletal development caused by mutations in TGFBR1 or TGFBR2. **Nat Genet** **37**:275–281, 2005
 24. Malfait F, Coucke P, Symoens S, Loeyes B, Nuytinck L, De Paepe A: The molecular basis of classic Ehlers-Danlos syndrome: a comprehensive study of biochemical and molecular findings in 48 unrelated patients. **Hum Mutat** **25**:28–37, 2005
 25. Marin-Padilla M: Notochordal-basichondrocranium relationships: abnormalities in experimental axial skeletal (dysraphic) disorders. **J Embryol Exp Morphol** **53**:15–38, 1979
 26. Marin-Padilla M, Marin-Padilla TM: Morphogenesis of experimentally induced Arnold-Chiari malformation. **J Neurol Sci** **50**:29–55, 1981
 27. McKusick VA: Hereditary disorders of connective tissue. **Bull N Y Acad Med** **35**:143–156, 1959
 28. Milhorat TH, Chou MW, Trinidad EM, Kula RW, Mandell M, Wolpert C, et al: Chiari I malformation redefined: clinical and radiographic findings for 364 symptomatic patients. **Neurosurgery** **44**:1005–1017, 1999
 29. Miller JD, al-Mefty O, Middleton TH III: Synovial cyst at the craniocervical junction. **Surg Neurol** **31**:239–242, 1989
 30. Mor V, Laliberte L, Morris JN, Wiemann M: The Karnofsky Performance Status Scale. An examination of its reliability and validity in a research setting. **Cancer** **53**:2002–2007, 1984
 31. Nishikawa M, Sakamoto H, Hakuba A, Nakanishi N, Inoue Y: Pathogenesis of Chiari malformation: a morphometric study of the posterior cranial fossa. **J Neurosurg** **86**:40–47, 1997
 32. Nyland H, Krogness KG: Size of posterior fossa in Chiari type I malformation in adults. **Acta Neurochir (Wien)** **40**:233–242, 1978
 33. O'Brien MF, Casey AT, Crockard A, Pringle J, Stevens JM: Histology of the craniocervical junction in chronic rheumatoid arthritis: a clinicopathologic analysis of 33 operative cases. **Spine** **27**:2245–2254, 2002
 34. Onofrio BM, Mih AD: Synovial cysts of the spine. **Neurosurgery** **22**:642–647, 1988
 35. Owler BK, Halmagyi GM, Brennan J, Besser M: Syringomyelia with Chiari malformation; 3 unusual cases with implications for pathogenesis. **Acta Neurochir (Wien)** **146**:1137–1143, 2004
 36. Patel NP, Wright NM, Choi WW, McBride DQ, Johnson JP: Forestier disease associated with a retroodontoid mass causing cervicomedullary compression. **J Neurosurg** **96** (2 Suppl):190–196, 2002
 37. Pepin M, Schwarze U, Superti-Furga A, Byers PH: Clinical and genetic features of Ehlers-Danlos syndrome type IV, the vascular type. **N Engl J Med** **342**:673–680, 2000
 38. Puget S, Kondageski C, Wray A, Boddaert N, Roujeau T, Di Rocco F, et al: Chiari-like tonsillar herniation associated with intracranial hypotension in Marfan syndrome. Case report. **J Neurosurg** **106** (1 Suppl):48–52, 2007
 39. Pyeritz RE: The Marfan syndrome. **Annu Rev Med** **51**:481–510, 2000
 40. Rahimi SY, Stevens EA, Yeh DJ, Flannery AM, Choudhri HF, Lee MR: Treatment of atlantoaxial instability in pediatric patients. **Neurosurg Focus** **15**(6):ECP1, 2003
 41. Ranawat CS, O'Leary P, Pellicci P, Tsairis P, Marchisello P, Dorr L: Cervical spine fusion in rheumatoid arthritis. **J Bone Joint Surg Am** **61**:1003–1010, 1979
 42. Schady W, Metcalfe RA, Butler P: The incidence of cranio-cervical bony anomalies in the adult Chiari malformation. **J Neurol Sci** **82**:193–203, 1987
 43. Schwarze U, Atkinson M, Hoffman GG, Greenspan DS, Byers PH: Null alleles of the COL5A1 gene of type V collagen are a cause of the classical forms of Ehlers-Danlos syndrome (types I and II). **Am J Hum Genet** **66**:1757–1765, 2000
 44. Shen FH, Samartzis D, Jenis LG, An HS: Rheumatoid arthritis: evaluation and surgical management of the cervical spine. **Spine** **4**:689–700, 2004
 45. Smoker WR: Craniocervical junction: normal anatomy, craniometry, and congenital anomalies. **Radiographics** **14**:255–277, 1994
 46. Speer MC, Enterline DS, Mehlretter L, Hammock P, Joseph J, Dickerson M, et al: Chiari type I malformation with or without syringomyelia: prevalence and genetics. **J Genet Couns** **12**:297–311, 2003
 47. Steinmann B, Royce PM, Superti-Furga A: The Ehlers Danlos syndrome, in Royce PM, Steinmann B (eds): **Connective Tissue and Its Heritable Disorders: Molecular, Genetic, and Medical Aspects**. New York: Wiley-Liss, 1993, pp 351–407
 48. Sze G, Brant-Zawadzki MN, Wilson CR, Norman D, Newton TH: Pseudotumor of the craniocervical junction associated with chronic subluxation: MR imaging studies. **Radiology** **161**:391–394, 1986
 49. Vega A, Quintana F, Berciano J: Basichondrocranium anomalies in adult Chiari type I malformation: a morphometric study. **J Neurol Sci** **99**:137–145, 1990
 50. Wiesel SW, Rothman RH: Occipitoatlantal hypermobility. **Spine** **4**:187–191, 1979
 51. Yamaguchi I, Shibuya S, Arima N, Oka S, Kanda Y, Yamamoto T: Remarkable reduction or disappearance of retroodontoid pseudotumors after occipitocervical fusion. Report of three cases. **J Neurosurg Spine** **5**:156–160, 2006
 52. Yoshida M, Tamaki T, Kawakami M, Natumi K, Minamide H, Hashizume H: [Retro-odontoid pseudotumor associated with chronic atlanto-axial instability: pathogenesis and surgical treatment.] **Rinsho Seikeigeka** **30**:395–402, 1995 (Jpn)
 53. Zunkeler B, Schelper R, Menezes AH: Periodontoid calcium pyrophosphate dihydrate deposition disease: "pseudogout" mass lesions of the craniocervical junction. **J Neurosurg** **85**:803–809, 1996
 54. Zygmunt S, Säveland H, Brattström H, Ljunggren B, Larsson EM, Wollheim F: Reduction of rheumatoid periodontoid pannus following posterior occipito-cervical fusion visualised by magnetic resonance imaging. **Br J Neurosurg** **2**:315–320, 1988

Manuscript submitted June 11, 2007.

Accepted August 9, 2007.

This work was supported in part by the Intramural Research Program of the National Institutes of Health National Institute on Aging.

Address correspondence to: Thomas H. Milhorat, M.D., Department of Neurosurgery, The Chiari Institute, Harvey Cushing Institutes of Neuroscience, North Shore-LIJ Health System, 300 Community Drive, Manhasset, New York 11030. email: Milhorat@nshs.edu.